Reaction Chemistry & Engineering

ROYAL SOCIETY OF CHEMISTRY

PAPER

View Article Online
View Journal | View Issue

Cite this: *React. Chem. Eng.*, 2026, **11**, 228

An accessible and efficient 3D printed modular 'M-Arc' photoreactor

Rowan M. Bailey, [a] Mónica Martínez-Aguirre, [a] Bernd Schaefer, [b] Mark R. Crimmin [a] and Philip W. Miller *[a]

Received 5th September 2025,
Accepted 9th October 2025

DOI: 10.1039/d5re00395d

rsc.li/reaction-engineering

Photochemistry has recently re-emerged at the forefront of chemical development, however, access to affordable and reliable photoreactors that generate reproducible results is a continued challenge for researchers in the field. Herein we present an open-source 3D printable 'M-Arc' photoreactor, named for its modularity and internal arc structure. The M-Arc reactor features modular batch and flow reactor inserts, ports for one or two light sources and a fan unit for maintaining temperature control. The reactor was benchmarked against commercially available photoreactors using chemical actinometry and three classical photochemical transformations: photoisomerisation, dehalogenation and a cross-coupling amination reaction. Photon delivery in the M-Arc reactor was improved 3.25-fold compared to a commercial reactor which translated into enhanced rate of reaction for all three tested photoreactions. Using the flow reactor insert, a further rate improvement for photoisomerization was achieved, ultimately demonstrating a 15 times rate improvement *versus* the HepatoChem PhotoRedOx Box™ market product.

Introduction

Photochemistry has undergone a renaissance period in recent years following widespread access to narrow wavelength LED lamps.[1–4] Compared to historical, broad wavelength xenon/mercury lamps, LED technologies have granted chemists access to targeted wavelength excitation, reducing the risk of undesirable side reactions or photodegradation which has previously limited the scope of applications.[5] Consequently, photocatalysis has been broadly adopted in recent years, facilitating the development of novel chemical transformations using mild reaction conditions and visible light.[6–9] Access to light-mediated contra-thermodynamic reactions are of particular interest as they can facilitate otherwise inaccessible synthetic steps and support energy storage technologies.[10]

Given the contemporality of the photochemical field, many research groups publish reports using unique reaction set ups. This trend has limited capacity for reaction replication both internally and more broadly between research peers.[11] It is clear that reactor standardisation is necessary to overcome these issues and ultimately boost development of robust reactions.[12]

Standardised commercial products have partially addressed this issue, offering reliable and reproducible reactor geometries. However, their associated high costs often limit their accessibility to academic groups. Indeed, it is also the case that many commercially available photoreactors lack modularity to enable screening at different reactor volumes and scales. For example, the translation of batch reactions into flow regimes often requires the purchase of additional commercial products, further increasing expenses. Flow translation is an especially valuable tool for photochemical research as photon delivery falls off exponentially with reactor depth. Use of microfluidic tubing and flow regimes can neutralise this limitation, facilitating scalable photochemical processes.[13] Though photon delivery is often an underappreciated aspect of photochemistry, it has been highlighted as a key consideration in the mechanistic discovery of these systems.[14] Accordingly, the direct comparison of batch and flow reactivity in a single reactor geometry is invaluable, ideally while using the same, standardised, photon sources.[5]

3D printable photoreactor templates can address many of these issues.[15–28] The cost associated with 3D printing is often orders of magnitude lower compared with commercial products. Furthermore, many reactor geometries have been presented and benchmarked, granting flexibility and confidence in the design concepts. The high precision associated with 3D printing provides further robustness in reactor replication.[29] However, for many of these templates, the design concepts centralise around either batch or flow capabilities, with few examples demonstrating exchangeable access to both.

[a] *Department of Chemistry, Imperial College London, W12 0BZ, London, UK. E-mail: philip.miller@imperial.ac.uk*
[b] *BASF SE, RGR/CN - B009, Carl-Bosch-Strasse 38, 67056 Ludwigshafen am Rhein, Germany*

Herein we present a 3D-printed modular 'M-Arc' photoreactor capable of hosting multiple batch scales and flow reactions. Photon delivery of the M-Arc reactor is benchmarked against two commercially available reactors *via* ferrioxalate based actinometry.[30] Kinetic study of three photocatalytic reactions, namely the photoisomerization of *trans*-stilbene, dehalogenation of phenacyl bromide and a dual-photocatalytic amination of aryl bromide showed improved rates of reaction using the M-Arc reactor *versus* alternative geometries.[31–33] Furthermore, using the flow insert, a comparison was made between the kinetics of the batch and flow photoisomerization reaction of *trans*-stilbene.

Results and discussion

System and optimisation

It was our aim to produce a simple, cost effective and accessible photoreactor that would require minimal engineering and importantly lead to reliable and reproducible photochemical results. Three key reactor characteristics were considered in the design concept and prototyping of the M-Arc photoreactor: (i) the reactor housing should be 3D printable as one complete unit, removing the need for further assembly. It should contain ports for readily accessible light sources and a fan for temperature regulation, (ii) a modular insert system should be designed that can enable batch and flow reactions (iii) a base stand should fit with many commercially available stirrer hotplates to ensure consistent mixing of batch reactions (Fig. 1).

We opted for a direct irradiation approach over reflective panelling, often seen in photoreactors, as it simplifies the set-up, shortens the photon path length and removes the variability that reflective surfaces can introduce *via* surface contamination. A carousel insert was designed to maintain equidistance between reaction vials and LED lamps which should support consistent and homogeneous light delivery to all four vials (Fig. 1).

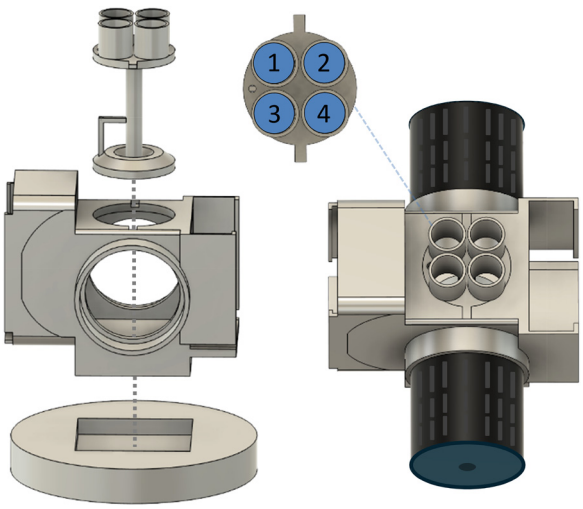

Fig. 1 M-Arc reactor schematic (left). Hotplate base (bottom), photoreactor housing (middle), vial carousel (4 × microwave vial example) (top). LED lamp mounting of Kessil or HepatoChem EvoluChem lamps (right).

Controlled stirring properties across all vial positions was important in the M-Arc reactor design to ensure consistent reaction mass transfer. Discrepancies in mixing properties, which have been observed in commercial and bespoke photoreactors, can lead to inconsistent reaction outcomes. The reactor base was designed to fit onto standard stirrer hotplates with 135 mm & 145 mm diameters, centralising both the reactor and carousel. By extension, the position of the reaction vials relative to the magnetic centre are equivalent, providing consistent stirring across all reactor positions.

Maintaining cool and constant reaction temperatures are key considerations for photochemical reactions to minimise thermally initiated side reactions and relaxation pathways of photocatalysts. Both commercial and bespoke systems can be limited for temperature control, leading to inconsistent photocatalyst activity and by-product formation. Prioritising temperature control for the M-Arc reactor, housing for an 80 × 80 mm fan was designed into the rear of the reactor to provide controllable, active cooling orthogonal to irradiation source. Through this, we envisaged that temperature control would be improved while also ensuring that light escape *via* the fan would be safely contained at the rear of the reactor. Airflow is diverted through the unique internal arc design, allowing hot exhaust gas to exit towards the top of the reactor (Fig. 2a). In some niche cases, application of heat can complement photochemical reactivity. To allow for flexible elevated temperature screening, a variable power fan was applied to provide a range of available operation temperatures. Benchmarking was conducted to confirm steady state reaction temperatures during irradiation. Vials were filled with water and 450 nm HepatoChem lamps (2 × 18 W) were used to irradiate the reactor vials. Solution temperatures were measured by an internal thermocouple each second to track heat removal (Fig. 2b).

Irradiative conditions with the fan switched off showed a steady state temperature of 55 °C. Subsequently, the integrated fan was switched on at variable power settings. At 12 W fan power, an *in situ* steady state temperature of 31 °C was achieved. 8 W and 4 W settings gave 34 °C and 37 °C reaction temperatures respectively. Impressively, steady state was reached within 10 minutes of fan initiation, suggesting that air flow provided by the fan was sufficient to stabilise the reactor. Given the relatively high specific heat capacity of our tested solvent, water, it is expected that heat removal may be even more efficient with conventional organic solvents. Simultaneous irradiation and cooling *via* the fan gave a steady state temperature of 33 °C. Variance compared to prior test is attributed to a higher ambient laboratory temperature.

As mentioned prior, modularity is an integral design feature necessary to reduce need for bespoke reactors. In the M-Arc reactor, the standard carousel design uses microwave crimp vials (ID = 12.0 mm, OD = 16.8 mm) as these are

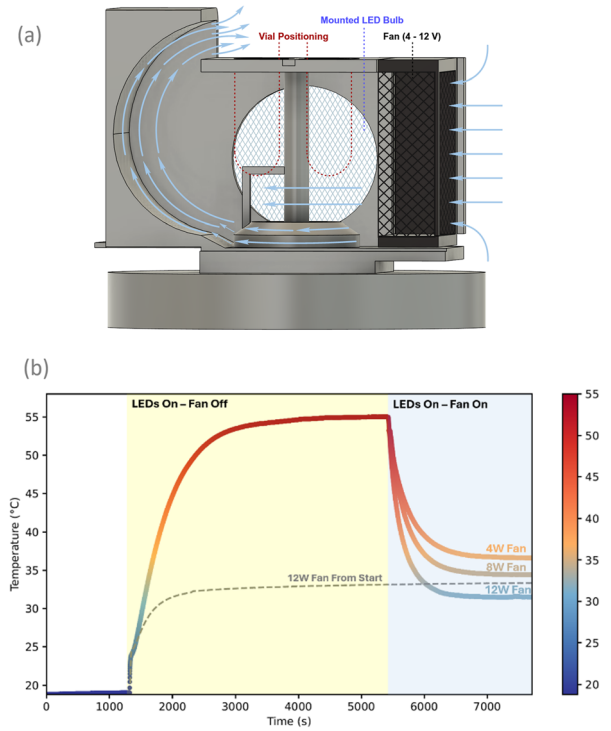

Fig. 2 (a) Implementation of internal arc geometry to aid with airflow in the M-Arc reactor. (b) Temperature profile of M-Arc photoreactor when irradiated with 450 nm LEDs (2 × 18 W). A variable voltage fan confirmed the influence of fan power with reactor steady state temperature.

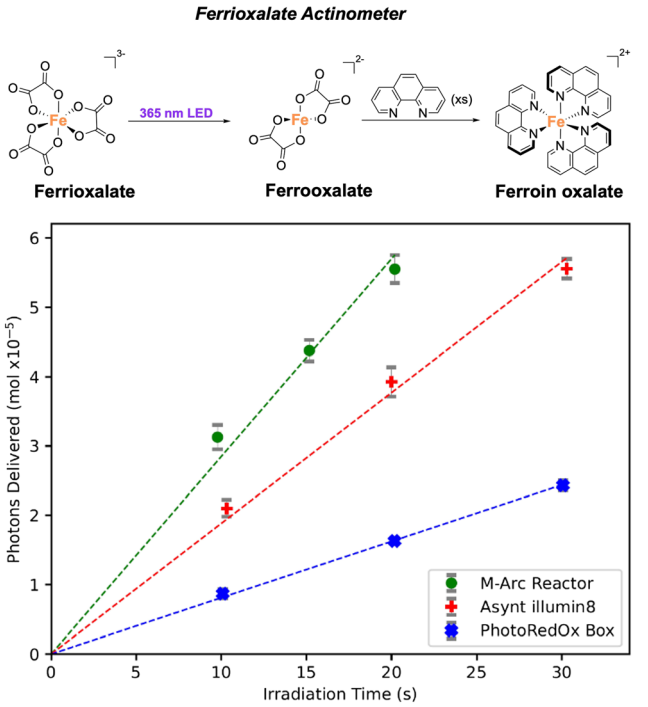

Fig. 3 Actinometric quantification of light delivery for M-Arc reactor and two commercial products (Asynt Illumin8 & HepatoChem PhotoRedOx Box™).

flexible to both air exclusion and pressurisation, enabling a range of chemical reactions. However, alternative designs are presented for application of NMR tubes, HPLC vials, UV-Cuvettes, Q-Tube™ reactor vessels and flow tubing (Fig. S3–S9). Ultimately, the design flexibility of the carousel is limited only by the space available in the reactor. Modular parts were designed with tight manufacturing tolerances to ensure minimal light loss and improve reactor safety. Light source modification is also supported by the M-Arc reactor. With a standard diameter of 64 mm, trusted HepatoChem and Kessil LED lamps fit tightly into the standard reactor geometry. Indeed, this feature is also readily adjustable to suit a range of alternative LED sources.

Reactor benchmarking – actinometric comparison

Photon delivery was tested in the M-Arc reactor *via* chemical actinometry to ensure that the direct irradiation concept could facilitate good light properties. A ferrioxalate chemical actinometer was used to quantify photon delivery using a HepatoChem EvoluChem™ LED (365 nm, 1 × 18 W) (Fig. 3). Vial positions 1 and 2 were irradiated simultaneously to confirm consistency (Fig. 1). Actinometric characterisation of two commercial photoreactors was acquired for comparison.

Using the same LED source and reactor vials, the M-Arc reactor delivered 3.25 times more photons to the ferrioxalate solution than the HepatoChem PhotoRedOx Box™ (1.6 *vs.* 0.5×10^{-5} mol s^{-1}), confirming direct irradiation was superior to reflective panelling for photon delivery in this case. Comparison with an Asynt Illumin8 photoreactor showed that the M-Arc reactor was again able to outperform a commercial product for photon delivery. However, the Illumin8 reactor uses bespoke LEDs and vials compared to the M-Arc and PhotoRedOx Box™, so direct comparison with this system is less reliable. Interestingly, the Asynt Illumin8 also compared favourably to the PhotoRedOx Box™ which relies on a set of internal mirrors for photon delivery. The Illumin8 reactor provides photons *via* direct irradiation, analogous to the M-Arc photoreactor, suggesting that the streamlined design philosophy may consistently outperform competitive reflection-based designs.

Reaction kinetics comparison study

The impact of improved photon delivery on chemical kinetics was investigated through three unique photocatalysed reactions. Modification of literature methodologies enabled application of 2,4,5,6-tetra(9*H*-carbazol-9-yl)isophthalonitrile (4-CzIPN) photocatalyst and 450 nm LEDs (1 × 18 W) in all tests to maintain consistency.[31–33] The first reaction tested was a classical isomerisation of *trans*-stilbene; second, a dehalogenation reaction of phenacyl bromide; and finally, a cross-coupling amination of 4-fluorobromobenzene with aniline, co-catalysed by [$NiBr_2$·glyme] (Fig. 4).

As expected, improved photon delivery led to a marked improvement in reaction kinetics across all tested reactions.

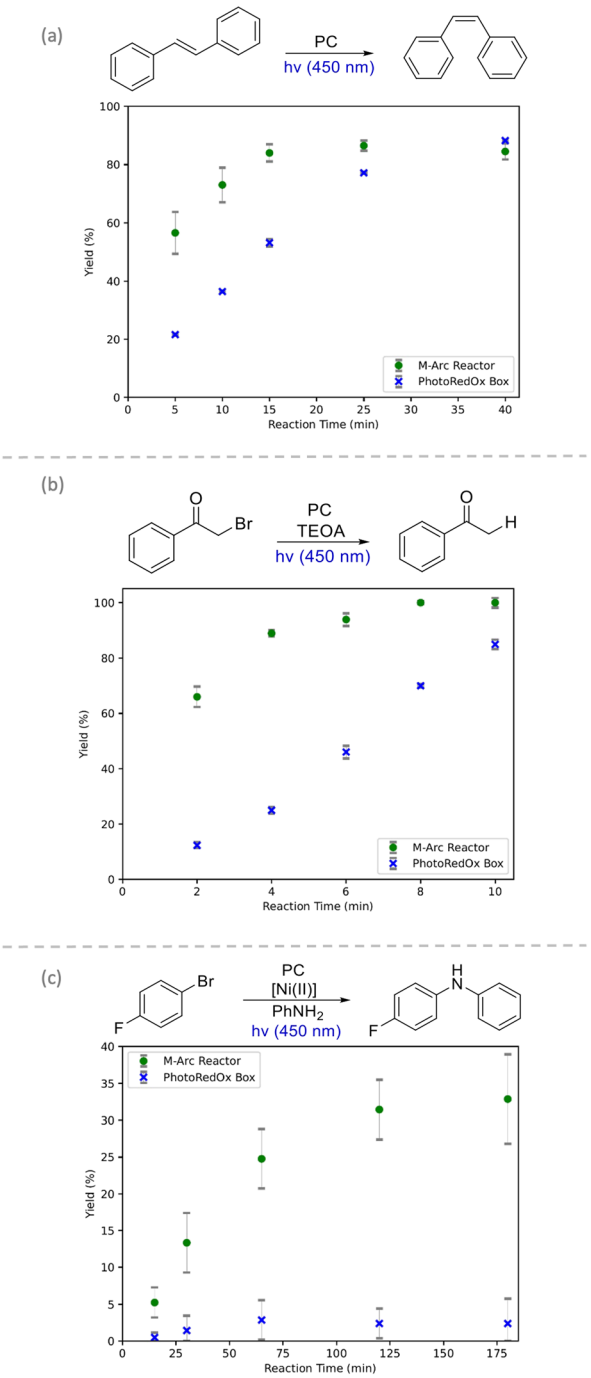

Fig. 4 Kinetic comparison of M-Arc reactor and HepatoChem PhotoRedOx Box™. Reactions completed in described microwave crimp vials (ID = 12.0 mm, OD = 16.8 mm). Reactor positions 1 & 2 irradiated simultaneously with one lamp to generate dataset & error bars calculated accordingly. (a) Isomerisation of *trans*-stilbene. *trans*-Stilbene (180 mg, 1 mmol), 4CzIPN (19.7 mg, 0.025 mmol, 2.5 mol%), DMF (0.2 M), 450 nm LED (1 × 18 W). (b) Dehalogenation of phenacyl bromide. Phenacyl bromide (498 mg, 2.5 mmol), triethanolamine (0.99 mL, 7.5 mmol), 4CzIPN (9.8 mg, 0.0125 mmol, 0.5 mol%), DMF (0.5 M), 450 nm LED (1 × 18 W). (c) Cross-coupling amination of 4-fluorobromobenzene with aniline. 4-Fluorobromobenzene (0.44 mL, 4 mmol), aniline (558 mg, 6 mmol), *t*-butylamine (0.9 mL, 5.2 mmol), $NiBr_2$·glyme (62 mg, 0.2 mmol, 5 mol%), 4CzIPN (15.8 mg, 0.02 mmol, 0.5 mol%), DMF (0.4 M) 450 nm LED (1 × 18 W).

For the isomerisation of *trans*-stilbene, *cis*-stilbene product was quantified in 57% yield after 5 minutes in the M-Arc reactor *versus* 22% in the PhotoRedOx Box™. Reaction completion was achieved in 15 and 40 minutes for the M-Arc and PhotoRedOx Box™ respectively. Initial rate comparison highlighted a 2.5-fold improvement using our presented reactor geometry (45.6 *vs.* 17.6 μmol min^{-1}). This reaction was also demonstrated at 0.5 mL (NMR) and 10 mL (Schlenk Flask) scale using alternative carousels (Fig. S20 and S21). At these two alternative scales, the rate of reaction again exceeded that of the commercial product.

In the second benchmarked reaction, the debromination of phenacyl bromide, a further enhancement to rate of reaction was demonstrated using the M-Arc reactor. An acetophenone yield of 66% was furnished after just 2 minutes of irradiation compared to a 12% yield for the commercial reactor. Initial rates of reaction were therefore improved by approximately 5.5 times in this case (330 *vs.* 60 μmol min^{-1}). The dehalogenation reaction reached completion within 10 minutes in the M-Arc reactor, however, was not complete within the same timeframe for the PhotoRedOx Box™.

The final reaction, a cross-coupling amination, displayed more complex reactivity patterns. Unlike the isomerisation and dehalogenation reactions, the nickel co-catalysed reaction gave rise to almost no product yield or starting material consumption in the commercial reactor. In contrast, a modest yield of ≈35% was observed in the M-Arc reactor. Given the greater complexity of this reaction compared to prior tests, the formation and lifetime of high energy radical intermediates may be more sensitive in this case, hence consistent photon delivery is more crucial for reactivity. Similarly, temperature control and stirring are especially important in this multicomponent system. Divergent reactivity highlighted the necessity for tighter reaction variable control which was ultimately demonstrated in the M-Arc reactor.

Flow translation – *trans*-stilbene isomerization

Flow reactions can offer greater reaction control while facilitating scale-up potential *versus* conventional batch reactions. As such, a growth in uptake of the technology has recently been applied in industrial settings.[34] Within photochemistry, microfluidic flow tubes have additional purpose in enhancing reaction surface area and light delivery properties. As seen prior, photon delivery is critical for both reactivity and rate of reaction. To afford flow reactivity in the M-Arc reactor, an interchangeable flow-carousel was designed, housing approximately 2.5 m of flow tubing with a 'figure-8' loop design (Fig. 5a). The kinetics of *trans*-stilbene isomerisation were investigated in flow. Reaction flow rates were selected to collect kinetic data for irradiation times between 15 seconds and 5 minutes (Fig. 5b).

The isomerisation of *trans*-stilbene in the M-Arc flow reactor was accelerated a further 6-fold in flow compared to

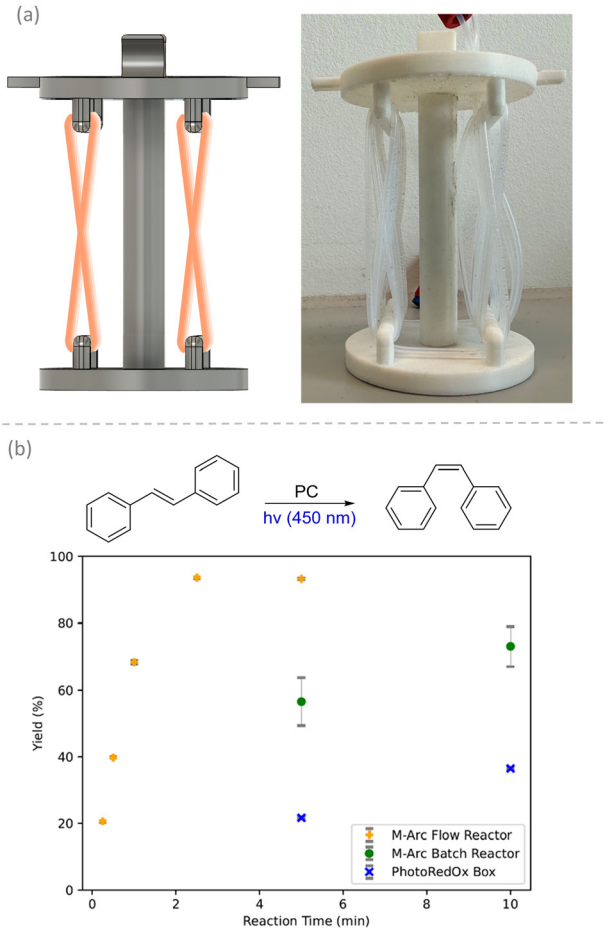

Fig. 5 (a) Figure-8 flow tubing fixation method (PTFE tubing, ID = 1.0 mm). (b) Kinetic uptake comparison of flow tubing in M-Arc reactor *versus* batch conditions in M-Arc and HepatoChem PhotoRedOx Box™.

the batch testing in a microwave vial (273 *vs.* 46 μmol min^{-1}), reaching completion in just 2.5 minutes (productivity = 3.0 g h^{-1}). Compared to the PhotoRedOx Box™, this represented an overall 15-fold improvement to rate of reaction (Fig. 5b). Evidently, translation to flow tubing and hence greater photon delivery efficiency can facilitate further improvement to rate of reaction while maintaining excellent consistency.

Conclusions

In conclusion, we present a new, open-source 3D-printable M-Arc photoreactor geometry. The reactor is carefully designed to address many common pitfalls observed with commercial and bespoke set-ups. Testing and characterisation of the M-Arc reactor showed excellent temperature control, consistent mixing and enhanced light delivery *versus* a commercial product. Kinetic benchmarking of the reactor showed the translation of these effects into photochemical reactions, where the M-Arc geometry accelerated reaction rates >5-fold. A flow carousel was designed and tested to supplement reactor characterisation. When applied to the isomerisation of *trans*-stilbene, flow reactions were a further 6 times faster than batch reactions, offering an overall 15-fold improvement to rate of reaction *versus* a commercial photoreactor. This reaffirmed the value of flow translation, and hence the need for access to flow capabilities. We therefore present the M-Arc reactor as an accessible, cost-effective and reliable system which also facilitates scaling and translation of batch reactions to flow regimes. We anticipate that the low cost and minimal technical barriers associated with this system will enable new and existing researchers in the field streamlined access to photochemical screening and research.

Conflicts of interest

The authors declare the following competing financial interest(s): R. M. B & P. W. M declare a financial interest for manufacture and distribution of M-Arc photoreactor.

Data availability

Open-source reactor files (.stl) are available *via* online repository: **https://github.com/RowanBailey99/M-Arc_Reactor** and in the SI.

Supplementary information: includes a detailed description of reactor design, experimental methods and key spectroscopic data. See DOI: **https://doi.org/10.1039/d5re00395d**.

Acknowledgements

This work utilised expertise and prototyping equipment at the Imperial College Advanced Hackspace. The authors are grateful to BASF SE for the financial support under the EPSRC REACT CDT Programme (EP/S023232/1) and to the EPSRC IConIC Prosperity Partnership (EP/X025292/1).

References

1 T. H. Rehm, *ChemPhotoChem*, 2020, **4**, 235–254.
2 J. D. Williams and C. O. Kappe, *Curr. Opin. Green Sustainable Chem.*, 2020, **25**, 100351.
3 F. Lévesque, M. J. Di Maso, K. Narsimhan, M. K. Wismer and J. R. Naber, *Org. Process Res. Dev.*, 2020, **24**, 2935–2940.
4 M. Sender and D. Ziegenbalg, *Chem. Ing. Tech.*, 2017, **89**, 1159–1173.
5 H. E. Bonfield, T. Knauber, F. Lévesque, E. G. Moschetta, F. Susanne and L. J. Edwards, *Nat. Commun.*, 2020, **11**, 804.
6 N. J. Gesmundo, A. J. Rago, J. M. Young, S. Keess and Y. Wang, *J. Org. Chem.*, 2024, **89**, 16070–16092.
7 T. J. DeLano, U. K. Bandarage, N. Palaychuk, J. Green and M. J. Boyd, *J. Org. Chem.*, 2016, **81**, 12525–12531.
8 P. Li, J. A. Terrett and J. R. Zbieg, *ACS Med. Chem. Lett.*, 2020, **11**, 2120–2130.
9 D. A. DiRocco, K. Dykstra, S. Krska, P. Vachal, D. V. Conway and M. Tudge, *Angew. Chem., Int. Ed.*, 2014, **53**, 4802–4806.

10 X. Li, S. Cho, J. Wan and G. G. D. Han, *Chem*, 2023, **9**, 2378–2389.
11 A. Slattery, Z. Wen, P. Tenblad, J. Sanjosé-Orduna, D. Pintossi, T. den Hartog and T. Noël, *Science*, 2024, **383**, eadj1817.
12 B. Pijper, L. M. Saavedra, M. Lanzi, M. Alonso, A. Fontana, M. Serrano, J. E. Gómez, A. W. Kleij, J. Alcázar and S. Cañellas, *JACS Au*, 2024, **4**, 2585–2595.
13 S. D. A. Zondag, D. Mazzarella and T. Noël, *Annu. Rev. Chem. Biomol. Eng.*, 2023, **14**, 283–300.
14 J. A. Malik, A. Madani, B. Pieber and P. H. Seeberger, *J. Am. Chem. Soc.*, 2020, **142**, 11042–11049.
15 G.-N. Ahn, M.-J. Kim, S.-J. Yim, B. M. Sharma and D.-P. Kim, *ACS Sustainable Chem. Eng.*, 2022, **10**, 3951–3959.
16 A. Riddell, P. Kvist and D. Bernin, *Rev. Sci. Instrum.*, 2022, **93**, 084103.
17 E. G. Gordeev, K. S. Erokhin, A. D. Kobelev, J. V. Burykina, P. V. Novikov and V. P. Ananikov, *Sci. Rep.*, 2022, **12**, 3780.
18 F. Schiel, C. Peinsipp, S. Kornigg and D. Böse, *ChemPhotoChem*, 2021, **5**, 431–437.
19 S. Rossi, M. V. Dozzi, A. Puglisi and M. Pagani, *Chem. Teach. Int.*, 2020, **2**, 20190010.
20 M. R. Penny and S. T. Hilton, *J. Flow Chem.*, 2023, **13**, 435–442.
21 M. Renner and A. Griesbeck, *J. Chem. Educ.*, 2020, **97**, 3683–3689.
22 T. Aubineau, J. Laurent, L. Olanier and A. Guérinot, *Chem.: Methods*, 2023, **3**, e202300002.
23 D. Kowalczyk, P. Li, A. Abbas, J. Eichhorn, P. Buday, M. Heiland, A. Pannwitz, F. H. Schacher, W. Weigand, C. Streb and D. Ziegenbalg, *ChemPhotoChem*, 2022, **6**, e202200044.
24 G. Glotz and C. O. Kappe, *React. Chem. Eng.*, 2018, **3**, 478–486.
25 F. Zhao, D. Cambié, J. Janse, E. W. Wieland, K. P. L. Kuijpers, V. Hessel, M. G. Debije and T. Noël, *ACS Sustainable Chem. Eng.*, 2018, **6**, 422–429.
26 D. Cambié, F. Zhao, V. Hessel, M. G. Debije and T. Noël, *Angew. Chem., Int. Ed.*, 2017, **56**, 1050–1054.
27 J. W. Rackl, A. F. Müller, C. Bärtschi and H. Wennemers, *Helv. Chim. Acta*, 2024, **107**, e202400154.
28 T. M. Masson, S. D. A. Zondag, J. H. A. Schuurmans and T. Noël, *React. Chem. Eng.*, 2024, **9**, 2218–2225.
29 J. M. Aguirre-Cortés, A. I. Moral-Rodríguez, E. Bailón-García, A. Davó-Quiñonero, A. F. Pérez-Cadenas and F. Carrasco-Marín, *Appl. Mater. Today*, 2023, **32**, 101831.
30 B. Vandekerckhove, N. Piens, B. Metten, C. V. Stevens and T. S. A. Heugebaert, *Org. Process Res. Dev.*, 2022, **26**, 2392–2402.
31 M. A. Bryden, F. Millward, T. Matulaitis, D. Chen, M. Villa, A. Fermi, S. Cetin, P. Ceroni and E. Zysman-Colman, *J. Org. Chem.*, 2023, **88**, 6364–6373.
32 J. Düker, M. Philipp, T. Lentner, J. A. Cadge, J. E. A. Lavarda, R. M. Gschwind, M. S. Sigman, I. Ghosh and B. König, *ACS Catal.*, 2025, **15**, 817–827.
33 K. L. Materna and L. Hammarström, *Chem. – Eur. J.*, 2021, **27**, 16966–16977.
34 R. Porta, M. Benaglia and A. Puglisi, *Org. Process Res. Dev.*, 2016, **20**, 2–25.